Atmospheric Environment 155 (2017) 189–198

Contents lists available at ScienceDirect

Atmospheric Environment

journal homepage: www.elsevier.com/locate/atmosenv

Designing efficient nitrous oxide sampling strategies in agroecosystems using simulation models

Debasish Saha [a, *], Armen R. Kemanian [b], Benjamin M. Rau [c], Paul R. Adler [d], Felipe Montes [b]

[a] Ecosystem Science and Management, The Pennsylvania State University, University Park, PA 16802, United States
[b] Plant Science, The Pennsylvania State University, University Park, PA 16802, United States
[c] USDA Forest Service, Savannah River Forestry Sciences Lab, 241 Gateway Drive, Aiken, SC 29803, United States
[d] USDA-ARS-Pasture Systems and Watershed Management Research Unit, University Park, PA 16802, United States

HIGHLIGHTS

- Nitrous oxide flux estimated from discrete measurements have unknown uncertainty.
- This uncertainty is location-specific for regular-interval sampling.
- Rule-based sampling yields better and less costly estimates than regular sampling.
- The performance of rule-based sampling is location and system specific.

GRAPHICAL ABSTRACT

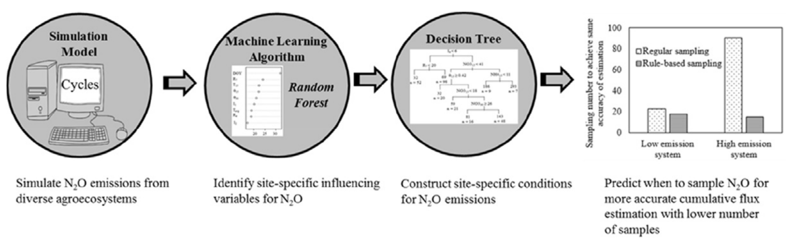

ARTICLE INFO

Article history:
Received 23 November 2016
Received in revised form
30 January 2017
Accepted 30 January 2017
Available online 31 January 2017

Keywords:
Cumulative nitrous oxide flux
Simulation model
Sampling
Fixed interval
Rule-based
Decision tree

ABSTRACT

Annual cumulative soil nitrous oxide (N_2O) emissions calculated from discrete chamber-based flux measurements have unknown uncertainty. We used outputs from simulations obtained with an agroecosystem model to design sampling strategies that yield accurate cumulative N_2O flux estimates with a known uncertainty level. Daily soil N_2O fluxes were simulated for Ames, IA (corn-soybean rotation), College Station, TX (corn-vetch rotation), Fort Collins, CO (irrigated corn), and Pullman, WA (winter wheat), representing diverse agro-ecoregions of the United States. Fertilization source, rate, and timing were site-specific. These simulated fluxes surrogated daily measurements in the analysis. We "sampled" the fluxes using a fixed interval (1–32 days) or a rule-based (decision tree-based) sampling method. Two types of decision trees were built: a high-input tree (HI) that included soil inorganic nitrogen (SIN) as a predictor variable, and a low-input tree (LI) that excluded SIN. Other predictor variables were identified with Random Forest. The decision trees were inverted to be used as rules for sampling a representative number of members from each terminal node. The uncertainty of the annual N_2O flux estimation increased along with the fixed interval length. A 4- and 8-day fixed sampling interval was required at College Station and Ames, respectively, to yield ±20% accuracy in the flux estimate; a 12-day interval rendered the same accuracy at Fort Collins and Pullman. Both the HI and the LI rule-based methods provided the same accuracy as that of fixed interval method with up to a 60% reduction in sampling events, particularly at locations with greater temporal flux variability. For instance, at Ames, the HI rule-based and the fixed interval methods required 16 and 91 sampling events, respectively, to achieve the same absolute bias of 0.2 kg N ha^{-1} yr^{-1} in estimating cumulative N_2O flux. These results suggest that

List of abbreviations: RF, Random Forest; DOY, day of year; T_{avg}, average air temperature; R, cumulative rainfall (and irrigation); I, net water inflow; SIN, total soil inorganic nitrogen; T, soil temperature; θ, volumetric soil water; HI, high input rule-based; LI, low input rule-based.

* Corresponding author.
E-mail address: debasish992@gmail.com (D. Saha).

http://dx.doi.org/10.1016/j.atmosenv.2017.01.052

using simulation models along with decision trees can reduce the cost and improve the accuracy of the estimations of cumulative N_2O fluxes using the discrete chamber-based method.

1. Introduction

Nitrous oxide (N_2O), a potent greenhouse gas (GHG), is mostly emitted from agricultural soils (IPCC Climate Change, 2007). This gas is produced through microbe-mediated processes, chiefly nitrification and denitrification (Firestone and Davidson, 1989). The temporal patterns of N_2O fluxes from agricultural soils are highly variable due to their episodic and transient nature, with marked diurnal and seasonal variations (Jacinthe and Dick, 1997; Smith et al., 2001; Flessa et al., 2002; Parkin, 2008). These emission events may occur in response to rainfall, irrigation, thawing, tillage, nitrogen (N) fertilization, and organic matter addition (Clayton et al., 1997; Oates et al., 2016; Reeves et al., 2016). Peak emission events can contribute about half of the growing season N_2O flux (Parkin and Kaspar, 2006). The high temporal variability makes the estimation of cumulative N_2O flux uncertain if measurements are not frequent or continuous (Parkin, 2008). However, assessing the impact of different management practices on N_2O emissions requires an accurate estimation of the cumulative flux.

In addition to the temporal variation, N_2O emissions vary spatially (Saha et al., 2016). Both time and space variations in N_2O fluxes are regulated by soil oxygen concentration (Smith and Dobbie, 2001), soil temperature (Parkin and Kaspar, 2006; Zhang et al., 2016), carbon (C) and mineral-N availability (Gillam et al., 2008), and microbial diversity (Regan et al., 2011). Weather conditions alter all these factors, causing a marked inter-year variability of N_2O fluxes from the same soil and management practices (Dobbie et al., 1999; Burchill et al., 2014). Since we have a limited ability to predict how these factors will drive N_2O emissions, sampling at representative times with time-discrete monitoring methods is challenging.

Soil N_2O flux is commonly measured by the non-steady state closed chamber method (Hutchinson and Mosier, 1981). This method is temporally discontinuous and usually applied on weekly to monthly fixed intervals (Dobbie and Smith, 2003). Low frequency sampling can miss a short-lived peak in-between sampling events, which will cause an underestimation of the cumulative flux. Thus, sampling at regular weekly or bi-weekly intervals does not ensure an accurate estimation of cumulative N_2O flux (Barton et al., 2015). It also adds samplings in periods with little N_2O emission. Furthermore, the same fixed interval sampling may produce a different uncertainty in cumulative flux estimates in different locations (Barton et al., 2015), or in the same location in different years, a variation that is as yet unknown. Automated chambers (Smith and Dobbie, 2001) and micrometeorological techniques (Wagner-Riddle and Thurtell, 1998) can provide high frequency measurements. However, these are expensive and have low spatial resolution which limits their use in plot-scale replicated studies or remote areas.

What is the best way to define an N_2O flux sampling strategy that minimizes uncertainty and cost in a given location? We propose to answer this question by a novel approach of using an agroecosystem simulation model as a tool to determine the error of different sampling strategies in estimating cumulative N_2O flux in a given location and set of management practices. Simulation models of agroecosystems typically operate on a daily or sub-daily time step, providing detailed outputs of the water and N balance components in the soil-plant system for many years. As long as the models satisfactorily represent the N_2O emission patterns and their drivers, the results can be conceived as surrogates of daily chamber-based flux measurements. The simulation outputs can be "sampled" with different strategies and determine which ones render the lowest uncertainty and cost at a given location and management system.

We further propose to apply statistical methods such as Classification and Regression Trees (CART, Breiman et al., 1984) and Random Forests (RF) (Breiman, 2001; Liaw and Wiener, 2002) to the daily simulation output to cluster the daily N_2O fluxes into groups that can be identified by specific properties (for example, precipitation, evapotranspiration or N fertilization rate in prior days). These properties can become rules for sampling, leading to a decision support tool for field N_2O monitoring. This strategy is hereafter referred to as rule-based sampling.

Our goal is to combine the output of simulation models with statistical methods to design a robust strategy for N_2O sampling that is less expensive than regular fixed interval sampling. The research questions are: 1) How do different fixed interval sampling frequencies affect the uncertainty in estimating cumulative N_2O flux? 2) Does the relative error of a given sampling frequency vary across soil, climate, and management scenarios? 3) Is it possible to use simulation models to build decision tree based N_2O sampling strategies that are cost effective? To answer these questions, we simulated and analyzed N_2O emissions in four sites in the United States (US) with diverse soil, climate, management practices, and temporally distinct N_2O emission patterns.

2. Materials and methods

2.1. Cycles model description

Cycles is a process-based, multi-year, multi-crop, and multi-soil layer simulation model that runs at a daily time step, with hydrology simulated with an adaptive sub-daily time step. It produces daily outputs of N_2O flux along with other biogeochemical fluxes. Cycles has modules to represent plant growth based on radiation and transpiration use efficiency (Stöckle et al., 2008), coupled soil C and N cycling (White et al., 2014), soil water infiltration and redistribution, and the effect of management practices on biogeochemical processes. Cycles can simulate monoculture rotations, polycultures, and relay crops. The inputs required to run Cycles are: i) latitude, elevation, and daily weather data, ii) layer-by-layer initial soil profile properties (layer thickness, texture, bulk density, hydraulic properties, organic matter), iii) crop sequence, and iv) management operations (fertilization, irrigation, residue addition, tillage, harvest). Earlier tests of CropSyst (Stöckle et al., 2003) and C-Farm (Kemanian and Stöckle, 2010) are applicable to Cycles as they share several modules; however, the N_2O emission algorithm in Cycles has been modified recently to accommodate N_2O emissions from nitrification.

Cycles simulates N_2O flux from nitrification and denitrification. For each soil layer, the amount of N_2O derived from nitrification depends on the amount of ammonium nitrified and the air filled porosity, which is calculated from soil porosity and volumetric water content. The N_2O derived from denitrification depends on the amount of N denitrified, nitrate concentration, aeration factor, and microbial respiration. The aeration factor is a power function of the layer air filled porosity and clay concentration.

2.2. Simulated sites description

We selected four sites in the US: Ames, IA (Midwest corn-belt); College Station, TX (east central Texas plains); Fort Collins, CO (irrigated high plains), and Pullman, WA (rainfed wheat production in the Columbia Plateau). For two of the sites, Ames (Jarecki et al., 2008; Parkin, 2008) and Fort Collins (Halvorson and Del Grosso, 2013), there are published records of N_2O fluxes along with soil N, water, and management practices, which allows validating the simulated results. For College Station and Pullman, common management practices were followed. Temperature and precipitation were obtained from NOAA stations at each location. The dew point temperature was assumed to be the minimum temperature. Solar radiation and wind speed were obtained from NASA's Prediction of Worldwide Energy Resources (NASA/POWER; power.larc.nasa.gov). Ames has a humid continental climate with cold winter; College Station is subtropical, with mild winter and warm and hot summer with highly variable and intense rainfall events; Fort Collins is semi-arid with lower precipitation, mostly in the summer; and Pullman is semi-arid with dry summer and wet fall, winter, and spring (Table S1). An initial soil profile database was obtained from the National Cooperative Soil Characterization Database (http://ncsslabdatamart.sc.egov.usda.gov). Major soil types according to USDA classification system were Canisteo clay loam (Typic Endoaquolls) at Ames, Burleson silty clay loam (Typic Endoaquolls) at College Station, Fort Collins clay loam (Aridic Haplustalf) at Fort Collins, and Palouse silt loam (Ultic Haploxerolls) at Pullman. The sites that were simulated varied in soil organic matter (range 20–45 g kg^{-1}) and clay content (range 170–400 g kg^{-1}) in the top 15 cm soil layer (Table 1). At Ames, chisel plowed and band-fertilized, rainfed corn (*Zea mays* L.) was rotated with soybean (*Glycine max* L.). At College Station, corn was followed by a winter cover crop (*Vicia* spp). The agroecosystem at Fort Collins was continuous corn conventionally tilled, fertilized, and irrigated. At Pullman, the system was rainfed, fertilized, continuous winter wheat (*Triticum aestivum* L.). Detailed site descriptions are given in Table 1.

2.3. Fixed interval sampling

The fixed interval sampling strategy consisted of (virtual) samples of daily outputs of soil N_2O flux for a year at regular time intervals, ranging from 1 to 32 days. The number of samples depends on the sampling interval. Linear interpolation between consecutive samples and integration provided an estimated annual N_2O flux. The estimate was then compared with the simulated 'actual' cumulative flux, obtained by sampling every day. For Ames and Fort Collins, we applied the fixed interval sampling strategy on the years with published N_2O flux measurements.

2.4. Rule-based sampling

The objective of rule-based sampling was to distribute the sampling events to balance peak and background emissions. Since N_2O emissions from soil are highly non-linear and have complex relationships with its controlling variables, we used RF on the simulated data to identify the important variables driving N_2O emissions at each location. These variables were used to construct a regression tree, which becomes the blueprint of the rule-based sampling strategy. The trees were independently developed for each location, as follows.

2.4.1. Selection of variables

The randomForest function from the package *randomForest* in R statistical software (Breiman, 2001; Liaw and Wiener, 2002) was used to determine the variable importance scores. The control parameters for RF were *seed* = 500 (set random number), *ntree* = 500 (number of trees), and *mtry* = $n^{0.5}$ (number of variables used at each split; n is the number of explanatory variables) (Strobl et al., 2009).

We applied RF on 15 years of simulated (training) data. To make it useful in practice, we selected variables that are plausible to be measured or generated with an automated algorithm in N_2O emission studies. These variables are: Calendar day (DOY), average

Table 1
Characterization of the four sites and agroecosystems. Soil properties are given for the top 15 cm.

Parameters	Simulated sites			
	Ames	College Station	Fort Collins	Pullman
Location				
Latitude	42°N	30.58°N	40.6°N	47°N
Longitude	93.6°W	95.6°W	105°W	117.1°W
Ecoregion	Western corn belt plains	East central Texas plains	High plains	Columbia plateau
Soils				
Type	Canisteo clay loam	Burleson Silty clay loam	Fort Collins clay loam	Palouse silt loam
USDA Classification	Typic Endoaquolls	Typic Endoaquolls	Aridic Haplustalf	Ultic Haploxerolls
Clay (g/kg)	230	400	340	170
Sand (g/kg)	370	130	400	190
Silt (g/kg)	400	470	260	640
Org. matter (g/kg)	45	24	20	32
Management practices				
Cropping system	Corn-soybean	Corn-*Vicia*	Continuous Corn	Winter wheat
Tillage	Chiesel-plow	Conventional-till	Conventional-till	Conventional-till
N-fertilization	Anhydrous NH_3 @ 168 kg-Nha^{-1} in Nov.	UAN @ 64 and 56 kg-N ha^{-1} in March and April	Urea @ 202 kg-N ha^{-1} in May and 23 kg N as NO_3 from irrigation water	Urea @ 92 kg-N ha^{-1} in April and 92 kg N ha^{-1} as UAN in Oct.
Application mode	Banding at 20-cm depth	Incorporation	Broadcasting	1st split broadcast and 2nd split incorporation
Irrigation	NA	NA	Scheduled sprinkler irrigation (460 mm)	NA

air temperature (T_{avg}, °C), cumulative rainfall (and irrigation) on the sampling day (R_1) or the 2–7 preceding days ($R_2 \ldots R_7$, mm), net water inflow or the difference between precipitation and evapotranspiration for the sampling day (I_1) or the 2–7 preceding days ($I_2 \ldots I_7$, mm; it assumes no runoff), soil NO_3 content in the 0–15 and 15–30 cm layer ($NO3_{15}$ and $NO3_{30}$; kg N ha^{-1}), soil NH_4 content in the 0–15 and 15–30 cm layer ($NH4_{15}$ and $NH4_{30}$; kg N ha^{-1}), total soil inorganic N in 0–15, 15–30, and 0–30 cm layer (SIN_{15}, SIN_{30}, and SIN_T; kg N ha^{-1}), volumetric soil water content in 0–15 and 15–30 cm layer (θ_{15} and θ_{30}; $m^3\ m^{-3}$), and soil temperature in 0–15 and 15–30 cm layer (T_{15} and T_{30}; °C).

From a practical point of view, the soil NO_3 and NH_4 content are not always available. To account for this reality, we used two types of rule-based sampling strategies. First, a high input rule-based sampling (HI) including the SIN related variables in the decision-making process. Second, a low input rule-based sampling (LI) that uses no SIN data. The analyses and tree building processes are the same for both HI and LI rule-based sampling.

2.4.2. Regression tree to predict N_2O flux

We used *rpart* package in R (*seed* = 500) to build the regression tree. Each tree was allowed to grow to its full length. We did not prune the trees, as pruning would have grouped nodes with low N_2O fluxes. Since the sampling selection process (presented below) is automatic, there is no penalty for not pruning. The algorithm does successive binary divisions ("rules") that generate terminal nodes, each having an average N_2O flux ($\bar{x}$) and number of members (n). Fig. 5a illustrates the derivation of each parameter for rule-based sampling. The total N_2O flux from each terminal node (F_i) is:

$$F_i = n_i \times \bar{x}_i \tag{1}$$

Where i identifies the terminal node (from 1 to N). The total N_2O flux (F_T) from N terminal nodes is:

$$F_T = \sum_{i=1}^{N} F_i \tag{2}$$

The proportion of flux contributed by each terminal node (P_i) to the F_T is:

$$P_i = \frac{F_i}{F_T} \tag{3}$$

2.4.3. Regression tree as a sampling decision aid

The tree so constructed can be used as the rule-based sampling strategy for a test year, i.e. a year excluded from the training dataset, since all the tree input information for a given day is known. Any day in a year corresponds to a tree node. The question is which day to sample. For this study, we assumed that we have resources to support 20-sampling events in a year. This is, of course, an arbitrary decision, but the generic question is: how do we temporally distribute any number of sampling events in a year? We allocated a number of sampling events to the i^{th} terminal node (T_i) based on its fractional contribution to the total flux (P_i, see Fig. 5a):

$$T_i = P_i \times 20 \tag{4}$$

Each day of the test year was run through the tree branches and assigned to a terminal node. The total number of days in a terminal node usually exceeds the number of possible samples (T_i) in that node. Therefore, the sampling days (T_i) were randomly selected from the group of days in i^{th} terminal node. The randomly selected days represent the days to measure N_2O flux in the field. The total flux under each node was calculated by multiplying the average flux of the randomly selected days and the frequency of days (n) of that terminal node in the test year. The sum of the fluxes from all terminal nodes in the test year gives the rule-based cumulative N_2O flux estimate. This process was repeated multiple times for the test year (because the specific sampling days are randomly selected within each terminal node) to obtain the estimation bias and to compare it with the bias of the fixed interval strategy for a given number of samples.

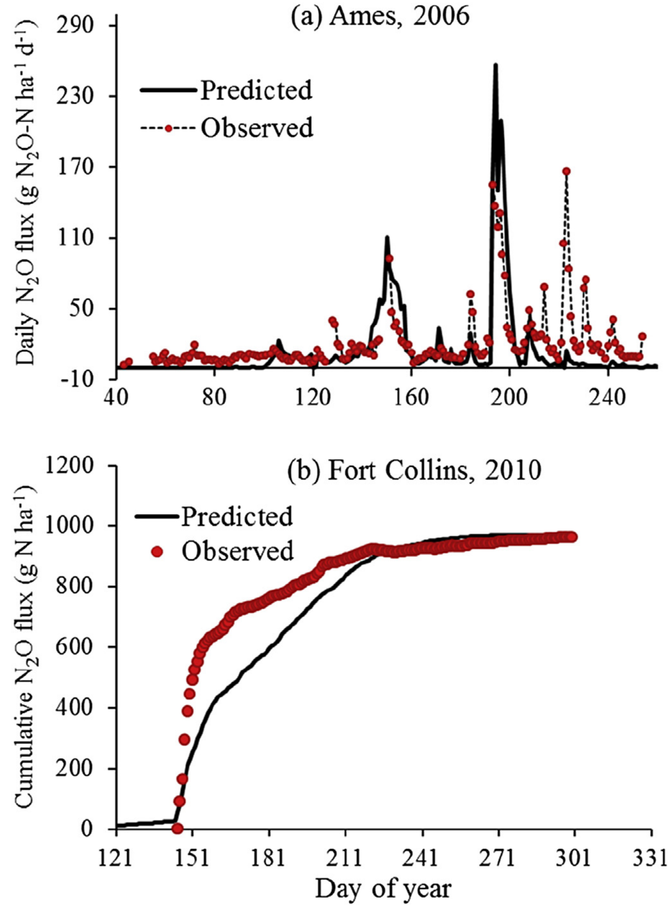

Fig. 1. Comparison of predicted and measured temporal N_2O emissions at (a) Ames and (b) Fort Collins in 2006 and 2010, respectively. The measured N_2O fluxes were adapted from Jarecki et al. (2008) for Ames and Halvorson and Del Grosso (2013) for Fort Collins. We used Web Plot Digitizer (Rohatgi, 2012) to extract the data published as figures in above articles.

3. Results

3.1. Cumulative soil N_2O emissions and model performance

The simulated cumulative N_2O flux differed greatly among the four locations in the test years (Table 2). It was highest at Ames, followed by College Station, Fort Collins, and Pullman, with fluxes of 3.2, 2.9, 1.0, and 0.4 kg N ha^{-1} y^{-1}. These are considered the 'actual' cumulative N_2O fluxes at each site.

The predicted cumulative flux at Ames in 2006 was lower than the reported 4.3 kg N ha^{-1} (Jarecki et al., 2008), yet within the 95% confidence interval. At that location, the model accurately predicted the temporal variability of N_2O emissions until DOY 223 of 2006 (Fig. 1a). However, the model did not predict any N_2O emission peak after DOY 210 (July 30) even though there were a few large precipitation events and peak emissions were reported

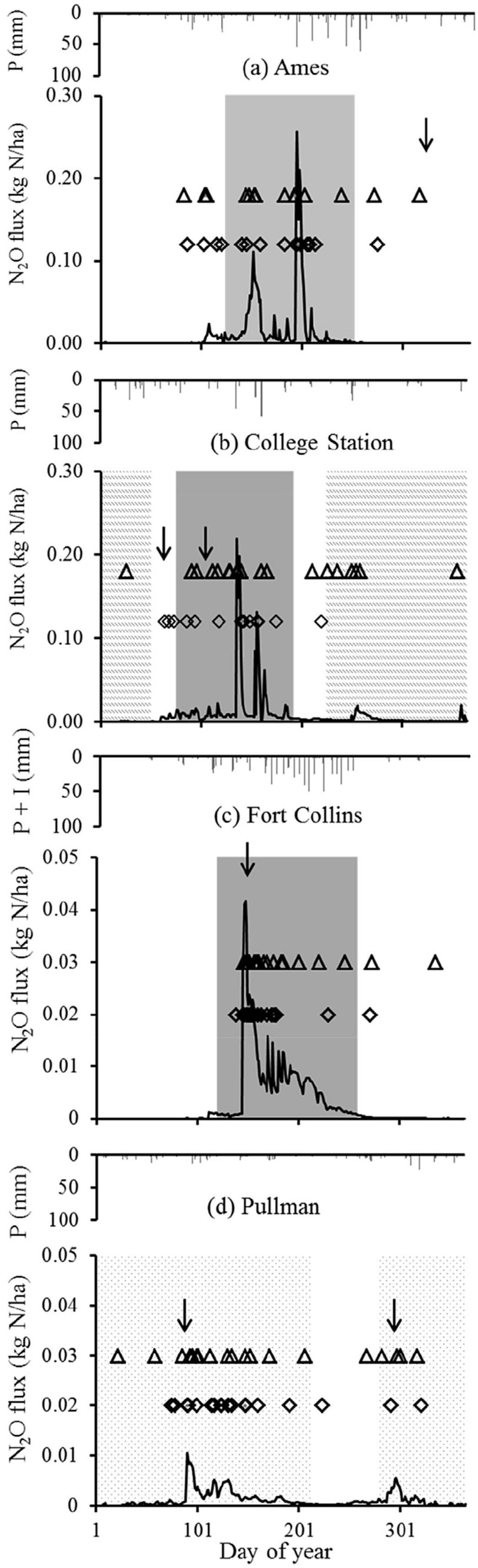

Fig. 2. Simulated daily N_2O flux (—) and gas sampling days as predicted by high-input (◊) and low-input (Δ) rule-based sampling at (a) Ames (2006), (b) College Station (2010), (c) Fort Collins (2010), and (d) Pullman (2013). The inverted graph on top of each panel shows daily precipitation (P) and irrigation (I). The arrow indicates the day of *N*-fertilization. The gray, dashed and dotted region in each panel represent the growing season of corn, cover crop (*Vicia* spp), and winter wheat, respectively.

(Parkin, 2008). The low modeled N_2O emissions after DOY 210 was due to SIN exhaustion via crop uptake and earlier N losses. This low SIN agrees with Jarecki et al. (2008), which makes difficult to explain the measured N_2O emissions.

At Fort Collins, the predicted cumulative flux of 1.0 kg N_2O–N ha^{-1} y^{-1} in 2010 was similar to that measured by Halvorson and Del Grosso (2013); however, the emissions were slightly underestimated immediately after fertilization (Fig. 1b).

3.2. Temporal patterns of N_2O emissions in the test years

Ames had a comparatively larger magnitude and time window of N_2O emissions with multiple emission peaks. A large precipitation event (≈55 mm) on DOY 192 initiated the largest emission window (DOY 192 to 202) with a peak of 256 g N ha^{-1} d^{-1} on DOY 194 (Fig. 2a). Although there were large precipitation events after DOY 202, emission peaks were relatively small on DOY 208 and 223 (43 and 15 g N ha^{-1} d^{-1}).

At College Station, the emission rate increased after the first *N*-fertilization (Fig. 2b). Several small emission peaks were simulated after the second *N*-fertilizer application on DOY 105, but the largest emission peak (220 g N ha^{-1} d^{-1}) was on DOY 136 in response to 46-mm of precipitation.

At Fort Collins, emissions were triggered by *N*-fertilizer application on DOY 145 and subsequent irrigation and precipitation events (Fig. 2c). The largest peak emissions (41 g N ha^{-1} d^{-1}) occurred shortly after fertilization and a 20-mm of irrigation on DOY 148. The N_2O emission gradually decreased as crop uptake gradually depleted the SIN pools.

With the lowest cumulative N_2O flux, emissions at Pullman were low throughout the test year 2013 and never exceeded 10 g N ha^{-1} d^{-1} (Fig. 2d).

3.3. Estimation of cumulative flux by fixed interval sampling

Increasing the interval between two sampling events increased the relative deviation from ‘actual’ (i.e. modeled) cumulative fluxes in a location-specific fashion. At Ames, relatively frequent sampling with a 4-day interval yielded a fairly accurate (±10%) cumulative flux estimate (Fig. 3a), but this accuracy degraded quickly as an 8-day interval sampling gave −16 to +26% of the expected flux. Comparative results were obtained at College Station (Fig. 3b). At sampling intervals greater than 12 days, the deviation in N_2O flux estimates exceeded ±100% of the actual cumulative flux. In contrast, at Fort Collins and Pullman a sampling frequency of once every 12 days produced an estimate of cumulative flux that is ±20% of the ‘actual’ one (Fig. 3c and d). The deviations from the ‘actual’ cumulative N_2O flux were least sensitive to sampling frequency at Pullman.

As expected, the absolute bias of cumulative flux estimation increased with increasing sampling interval, and was greatest at College Station and Ames followed by Fort Collins and Pullman (Fig. 4).

3.4. Estimation of cumulative flux by rule-based sampling

3.4.1. Variables important for N_2O emissions

The important variables that explained the variation in N_2O flux were location specific. When considering the HI predictors (i.e. including SIN), NO_3, θ, and precipitation explained most of the variation in emissions in the relatively moist environments of Ames and College Station (Fig. S1a and S1c), while NH_4 and temperature did so for the drier environments of Fort Collins and Pullman (Fig. S1e and S1g). When considering the LI predictors, DOY, and θ became the dominant variables at all locations; DOY becomes a surrogate for time since N fertilization. The percent of the variation in N_2O fluxes explained by RF degraded slightly from HI to LI, except in College Station where it dropped from 83 to 55%.

3.4.2. Regression tree for N_2O emissions

The tree for Ames is presented in detail illustrating each parameter of the rule-based sampling (Fig. 5), while the trees for the other locations are presented as supplemental material. The primary split of the HI tree for Ames was on $NO3_{15}$ (threshold 9 kg N ha^{-1}, Fig. 5a). Total inorganic N (SIN) and θ_{15} were also relevant variables. The largest but less frequent mean daily N_2O flux was predicted in terminal node 13 as 189 g N $ha^{-1}d^{-1}$, which results from moist soils (θ_{15} and θ_{30} > 20%) that receive a sizable precipitation (R_7 > 29 mm) and contain high $NO3_{15}$ (>36 kg N ha^{-1}). On the contrary, the tree for LI had a primary split between observations with T_{30} less than or more than 13 °C (Fig. 5b). Consistent with the LI-RF, the significance of DOY was preserved in the LI rule-based tree as it was the splitting variable four times in the tree. The HI and LI trees for College Station are similar to those for Ames, albeit with location-specific thresholds (Fig. S2a and S2b). Fort Collins had a relatively simple HI tree dominated by $NH4_{15}$, DOY, and T_{avg} (Fig. S2c), with higher N_2O emissions associated with *N*-fertilization. The LI tree simply dropped $NH4_{15}$, showing the maximum emission in the 5 days following fertilization (Fig. S2d). The trees for Pullman are comparable to those at Fort Collins (Fig. S2e and S2f). Unlike Ames and College Station, θ was not the major driver of N_2O emissions at Fort Collins or Pullman.

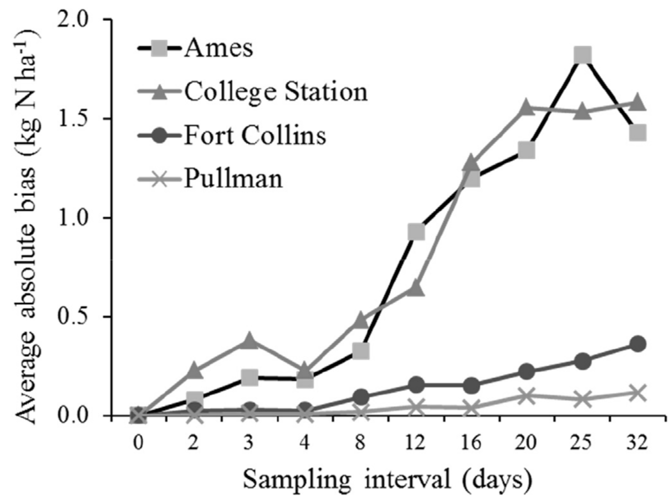

Fig. 4. Average absolute bias of cumulative flux estimation at different sampling frequencies by fixed interval sampling for the four studied locations.

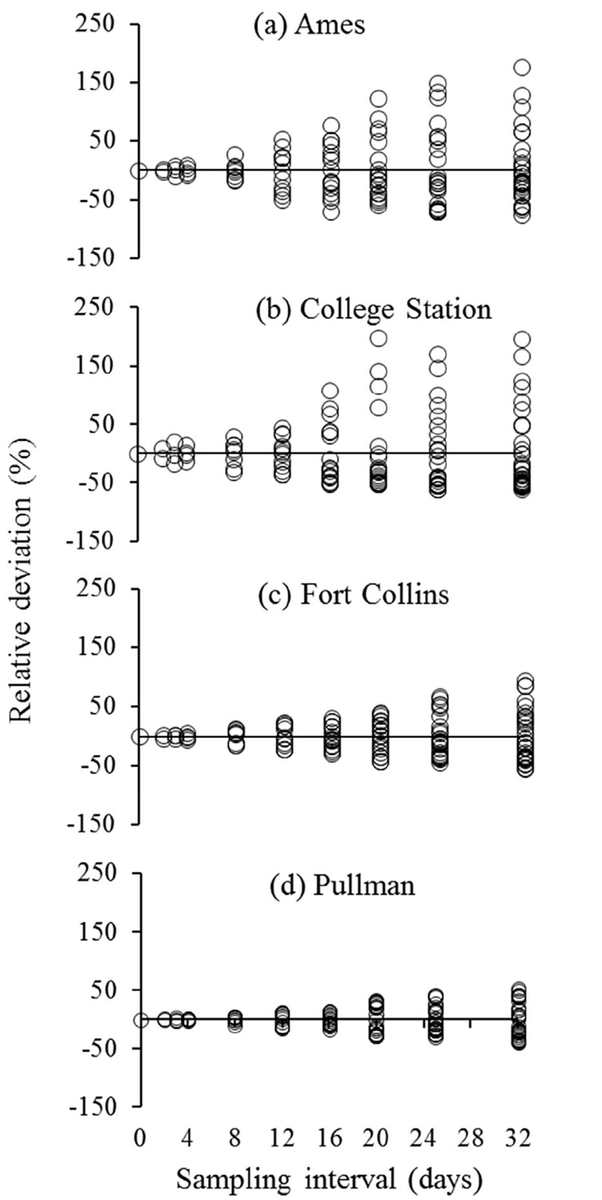

Fig. 3. Relative deviation of the estimated N_2O flux obtained with different fixed interval sampling at (a) Ames (2006), (b) College Station (2010), (c) Fort Collins (2010), and (d) Pullman (2013).

3.4.3. Prediction of sampling days by rule-based sampling

The predicted sampling events with both HI and LI trees at Ames were distributed over almost the same temporal window (Fig. 2a). The sampling events were responsive to the precipitation-induced peak N_2O emission from DOY 104 to 215, after which the N_2O emissions as well as HI sampling events were not responsive to the precipitation events. Intensive gas sampling was predicted to start on DOY 196 after receiving almost 70 mm of precipitation in the preceding four days and continued until DOY 215. For HI, a 44 mm of precipitation event on DOY 207 resulted in consecutive samplings in the next three days, but none by LI method.

At College Station, the HI sampling events started after the first split application of *N*-fertilizer followed by a 14 mm of precipitation on DOY 60, whereas intensive LI samplings started after DOY 90 and were distributed in a broader time window than HI samplings (Fig. 2b). Sampling became frequent from DOY 135 to 157, a period that included major precipitation and peak N_2O emission events during the corn growing period.

On the contrary, at Fort Collins, the sampling events were concentrated around the *N*-fertilization event on DOY 145 (Fig. 2c). However, LI samplings were more evenly spaced than HI sampling. The predicted sampling was frequent from DOY 145 to 163. At Pullman, both HI and LI rule-based sampling events were more evenly and widely distributed through the growing season (Fig. 2d). The split application of N on DOY 90 was associated with frequent sampling events.

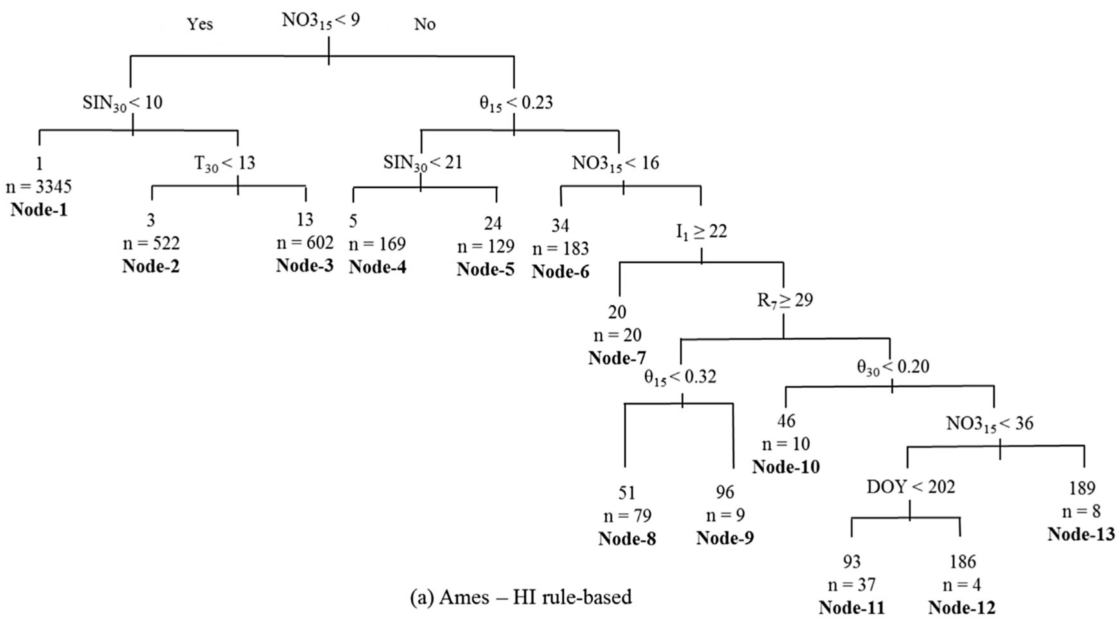

	Node 1	Node 2	Node 3	Node 4	Node 5	Node 6	Node 7	Node 8	Node 9	Node 10	Node 11	Node 12	Node 13
F_i[†]	1×3345 = 3345	3×522 = 1566	13×602 = 7826	5×169 = 845	24×129 = 3096	34×183 = 6222	20×20 = 400	51×79 = 4029	96×9 = 864	46×10 = 460	93×37 = 3441	186×4 = 744	189×8 = 1512
F_T	∑ 3345 + 1566 + 7826 + 845 + 3096 + 6222 + 400 + 4029 + 864 + 460 + 3441 + 744 + 1512												
P_i	$3345/F_T$	$1566/F_T$	$7826/F_T$	$845/F_T$	$3096/F_T$	$6222/F_T$	$400/F_T$	$4029/F_T$	$864/F_T$	$460/F_T$	$3441/F_T$	$744/F_T$	$1512/F_T$
T_i	P_1×20	P_2×20	P_3×20	P_4×20	P_5×20	P_6×20	P_7×20	P_8×20	P_9×20	P_{10}×20	P_{11}×20	P_{12}×20	P_{13}×20

[†]i ranges from 1 to 13 in this case

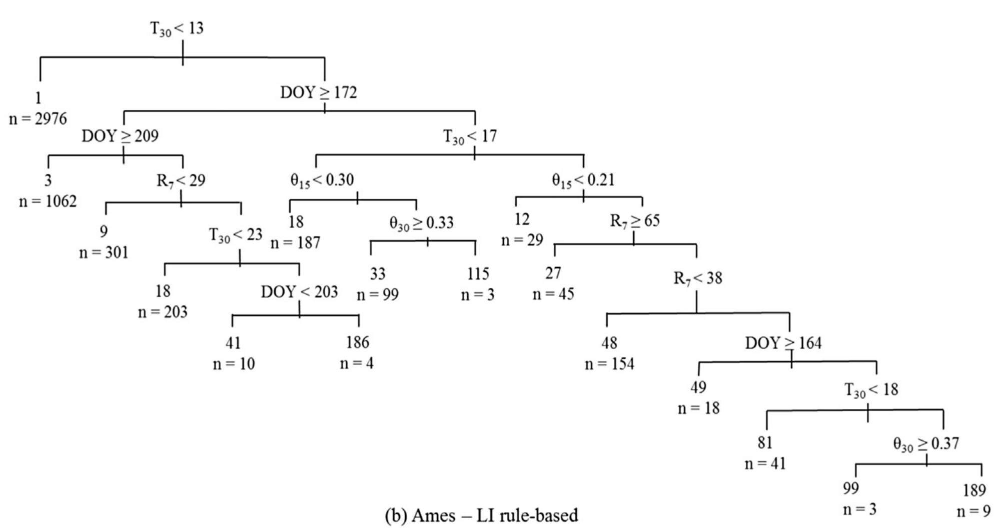

Fig. 5. High input (HI, a) and low input (LI, b) rule-based trees for Ames. Upon satisfaction of the splitting condition, the tree progresses to the left. Each terminal node reports the average N_2O flux (g N ha^{-1} d^{-1}) and number of observations (n). The representive table below Fig. 5a illustrates the derivation of each parameter of the rule-based sampling from the regression tree.

3.5. Comparison of rule-based and fixed interval sampling

Both HI and LI rule-based sampling strategies yielded reasonable estimates of cumulative N_2O flux with a substantially lower number of sampling events than fixed interval sampling (Table 2). The HI rule-based estimate at Ames in 2006 (3.1 kg

Table 2
Comparison of the rule-based and the fixed interval sampling methods skill at reproducing the simulated annual N_2O flux at four locations. For the rule-based sampling, the inclusion or exclusion of mineral N from the predicting variables is represented by high input (HI) or low input (LI).

Site	Year	Simulated flux	Cumulative Flux		Absolute bias		Number of sampling events		
			HI	LI	HI	LI	HI	LI	Fixed interval[a]
		kg N ha^{-1} y^{-1}	kg N ha^{-1} y^{-1}		kg N ha^{-1} y^{-1}				
Ames	2006	3.2	3.1	3.3	0.2	0.7	16	15	91
College Station	2010	2.9	3.0	2.7	0.2	0.3	14	19	186
Fort Collins	2010	1.0	1.1	0.9	0.1	0.1	19	20	37
Pullman	2013	0.4	0.4	0.4	0.05	0.04	18	18	23

[a] The number of sampling events by the fixed interval sampling was estimated from Fig. 3 based on the required sampling interval to achieve the absolute bias of HI rule-based sampling for the respective sites.

N_2O–N ha^{-1}) was within ±5% of the simulated cumulative flux (3.2 kg N_2O–N ha^{-1}) with only 16 sampling events; to obtain this accuracy with fixed interval sampling required 91 sampling events (Table 2 and Fig. 4). The LI rule-based sampling also yielded an estimate within ±5% of the expected N_2O cumulative flux (3.3 kg N_2O–N ha^{-1}). The HI rule-based method was even more efficient at College Station with only 14 sampling events to yield a cumulative estimate in 2010 of 3.0 kg N_2O–N ha^{-1}, within ±5% of the 'actual' cumulative flux (2.9 kg N_2O–N ha^{-1}). The fixed interval method needed 2-day interval samplings to achieve the same accuracy (Fig. 4). Similarly, the rule-based method at Fort Collins reduced the total sampling events from 37 to 19, to yield an estimate within ±10% accuracy of the cumulative flux (1.0 kg N_2O–N ha^{-1}). In contrast to other sites, at Pullman both the fixed interval and the rule-based sampling performed closely in terms of required number of sampling events to achieve the same bias (Table 2). The rule-based and fixed interval samplings used 18 and 23 sampling events, respectively. The significance of the absolute error of cumulative flux estimation is negligible at Pullman due to the low overall fluxes.

4. Discussion

While the importance of accurately estimating N_2O emissions from agricultural systems is widely recognized (Parkin and Kaspar, 2006), the dependence on the chamber-based method casts uncertainty on the reliability, practicality, and cost of this technique. This study proposed that a suite of simulation modeling and statistical approaches can help improve the timing of N_2O sampling, leading to a less costly and more accurate estimate of the cumulative N_2O flux. As shown in this research, the model can be used for this purpose because it predicted reasonably well the temporal variability of N_2O emission at Ames and Fort Collins (Fig. 1) along with N balance, and crop growth (Table S2) under different soil, climate, and management practices. Deviations from the measured N_2O emissions in the second half of the year 2006 at Ames are difficult to explain based on the low SIN level reported by Jarecki et al. (2008). It is possible that banding may have left pockets of high SIN in the soil under the chambers that cannot be easily simulated with the model nor measured without an intensive soil sampling.

When comparing Ames and College Station, it is instructive to consider how soil properties such as organic matter and clay content interact with N management and climate (Table 1 and Table S1, Fig. 2a and b). At both locations, the soil is likely to be moist in early spring. At Ames, the subsequent warming coupled with a soil with a high load of SIN in a band opens a wide window of time in which N_2O emissions can be sustained as long as leaching or crop uptake do not deplete SIN and the soil remains moist enough so that timely precipitation events trigger N_2O emissions. This mechanism underlies the relevance of SIN and θ in the variable importance plots and regression trees for these two sites (Fig. S1a, c, Fig. 5a, and Fig. S2a). The episodic nature of N_2O emissions is exacerbated at College Station because the soil dries faster due to the warmer climate, but convective storms and hurricanes can bring substantial precipitation quickly. When coupled with a clay soil that impedes drainage and causes soil saturation, the drying and sudden wetting can cause peak denitrification events. Accordingly, Asgedom et al. (2014) observed increased N_2O flux from vertisols after rainfall following *N*-fertilization. Sampling or not sampling one of these peaks can bias the estimation of the cumulative N_2O flux, a situation where a rule-based sampling can be most useful. Otherwise, a frequent sampling of 2–8 days interval would be needed at College Station and Ames to yield an estimate within ±20% of accuracy (Fig. 3a and b). These results obtained with a simulation model are remarkably similar to those reported by Parkin (2008) at Ames. Daily sampling has been recommended by Barton et al. (2015) in sites exhibiting extreme episodicity of N_2O emissions, but this is clearly not practical with the static chamber method.

On the contrary, at Fort Collins predictable peak emissions occur in response to precipitation and irrigation events soon after *N*-fertilization (Fig. 2c), a phenomenon observed in other studies (Dobbie et al., 1999; Baggs et al., 2003; Oates et al., 2016). Both the importance of the top layer NH_4 content on N_2O emissions in RF and the fact that NH_4 was the primary split on the regression tree (Fig. S1e and Fig. S2c) suggest that nitrification is the main source of the N_2O emission at Fort Collins, as observed in another relatively dry location in Montana by Engel et al. (2010). Thus, reasonable cumulative estimates of N_2O emission (within 20% of the actual flux) can be obtained with a relatively low intensity fixed interval sampling of once every two weeks (Fig. 3c). At Pullman, conditions are not prone for large emissions, and the relatively dry summer and cold winter probably caused lower N_2O emissions. In addition to relatively low precipitation, good soil drainage limits large emissions. However, there can be spatial hotspots of emissions since the Palouse is a landscape of rolling hills, where swales are wetter than ridgetops (Mulla et al., 1992) and runoff and subsurface flow may favor N_2O emissions from the swales. We did not address the spatial variation of soil moisture and N_2O emissions in this study. Frequent occurrences of air and soil temperature in the regression tree indicate the strong control of temperature on nitrification induced N_2O emissions. The lower temporal variability (Fig. 2d) allows an infrequent sampling (16 days interval) to achieve ±20% accuracy in the estimate (Fig. 3d). Furthermore, a ±20% error at Pullman is likely to result in a small absolute error as compared to ±20% error at Ames or College Station because the cumulative annual N_2O flux is comparatively low. The relatively low magnitude of the peak N_2O emissions at Fort Collins and Pullman suppressed the consequences of not sampling one of these peak events on the cumulative flux estimation. Reeves et al. (2016) similarly concluded that the influence of sampling schedule on the accuracy of estimation is lower in low emission systems. A given fixed interval sampling at contrasting sites may produce different errors of cumulative flux estimates, both in relative and absolute terms. This is due to different temporal patterns and the magnitude of N_2O emissions at different sites given the variation in soil, climate, and management practices (Flechard et al., 2007), which results in variations of the accuracy of the cumulative N_2O flux estimations, as clearly illustrated with these simulations.

The rule-based method performed better than the fixed interval strategy in estimating cumulative fluxes with a minimum number of sampling events at the four sites. The peak N_2O emission events usually comprise <5% of the time, thus the bias associated with infrequent fixed interval sampling could be large (Liengaard et al., 2014). It is therefore important to anticipate the occurrences of 'hot moments', which is what the rule based sampling accomplishes. This method not only allocates a greater proportion of the sampling events to the peak emission days and a lower proportion to the low, background emission days, but also provides a mean to weight the importance of each sampling event, yielding an overall estimate closer to the 'actual' cumulative flux. Reeves and Wang (2015) also suggested increasing the N_2O sampling frequency in a rain-fed cereal cropping system during rainfall events to achieve the same accuracy of estimation as in triweekly sampling. Our research provides a specific protocol to increase the sampling frequency when needed, and decrease it when sampling would be superfluous.

In general, soil moisture, SIN, and temperature were the critical factors for N_2O emissions, as reported in other studies (Dobbie et al., 1999; Davidson et al., 2000; Ma et al., 2010). The contribution of our research is that the specific thresholds for these variables at a given location and management system can be quantified to accommodate the distinct temporal variability of N_2O emissions at each site. When the N_2O flux variability is low, a low frequency fixed interval sampling can be adopted. Excluding SIN from the rule-based method (as in LI rule-based) did not have a substantial trade-off in the accuracy of estimation or increase in sampling numbers, an important result that makes this approach inexpensive and user-friendly (does not need SIN). The reason is not that SIN is not important, but that DOY surrogated its role explaining N_2O emissions (Fig. S1). However, this came at a cost of a wider temporal spread of the predicted sampling events in the LI rule-based method and a loss of accuracy in predicting 'hot moments' of N_2O emissions. Nonetheless, the LI rule based method still performed better than the fixed interval method, with better accuracy, time use, and cost savings on gas sampling and analysis.

5. Conclusions

The results showed that a simulation model that satisfactorily simulates variations in N_2O emissions could be a useful tool to assess the accuracy of sampling frequency in estimating cumulative flux. Increasing the sampling interval in a uniform sampling scheme increases the error of the cumulative flux estimation, but the magnitude of the error depends on the underlying temporal variability of N_2O emissions. When using a low frequency sampling, sites with greater temporal flux variability are at higher risk of large errors in the N_2O flux estimation. Estimation of cumulative N_2O flux by the rule-based sampling, with or without including the variables related to SIN, returns the best balance between total sample number and accuracy. This rule-based method can be a powerful tool to obtain accurate and cost effective estimations of cumulative N_2O fluxes, especially in systems with large variability of N_2O fluxes.

Acknowledgements

Funding for this research was provided by the USDOT SunGrant #52110-9601, USDA NIFA grant #2012-68005-19703, and USDA NIFA grant #2015-51106-24237.

Appendix A. Supplementary data

Supplementary data related to this article can be found at http://dx.doi.org/10.1016/j.atmosenv.2017.01.052.

References

Asgedom, H., Tenuta, M., Flaten, D.N., Gao, X., Kebreab, E., 2014. Nitrous oxide emissions from a clay soil receiving granular urea formulations and dairy manure. Agron. J. 106, 732–744.
Baggs, E.M., Stevenson, M., Pihlatie, M., Regar, A., Cook, H., Cadisch, G., 2003. Nitrous oxide emissions following application of residues and fertilizer under zero and conventional tillage. Plant Soil 254, 361–370.
Barton, L., Wolf, B., Rowlings, D., Scheer, C., Kiese, R., Grace, P., Stefanova, K., Butterbach-Bahl, K., 2015. Sampling frequency affects estimates of annual nitrous oxide fluxes. Sci. Rep. 5, 15912. http://dx.doi.org/10.1038/srep15912.
Breiman, L., 2001. Random forests. Mach. Learn 45, 5–32.
Breiman, L., Friedman, J.H., Olshen, R.A., Stone, C.J., 1984. Classification and Regression Trees. Wadsworth and Brooks/Cole, Monterey, California, USA.
Burchill, W., Li, D., Lanigan, G.J., Williams, M., Humphreys, J., 2014. Interannual variation in nitrous oxide emissions from perennial ryegrass/white clover grassland used for dairy production. Glob. Change Biol. 20, 3137–3146.
Clayton, H., McTaggart, I.P., Parker, J., Swan, L., Smith, K.A., 1997. Nitrous oxide emissions from fertilized grassland: a 2-year study of the effects of N fertilizer form and environmental conditions. Biol. Fertil. Soils 25, 252–260.
Davidson, E.A., Keller, M., Erickson, H.E., Verchot, L.V., Veldkamp, E., 2000. Testing a conceptual model of soil emissions of nitrous and nitric oxides. Bioscience 50, 667–680.
Dobbie, K.E., Smith, K.A., 2003. Nitrous oxide emission factors for agricultural soils in Great Britain: the impact of soil water-filled pore space and other controlling variables. Glob. Change Biol. 4, 204–218.
Dobbie, K.E., McTaggart, I.P., Smith, K.A., 1999. Nitrous oxide emissions from intensive agricultural systems: variations between crops and seasons, key driving variables, and mean emission factors. J. Geophys. Res. Atmos. 104, 26891–26899.
Engel, R., Liang, D.L., Wallander, R., Bembenek, B., 2010. Influence of urea placement on nitrous oxide production from a silt loam soil. J. Environ. Qual. 39, 115–125.
Firestone, M.K., Davidson, E.A., 1989. Microbiological basis of NO and N2O production and consumption in soil. In: Andreae, M.O., Schimel, D.S. (Eds.), Exchange of Trace Gases between Terrestrial Ecosystems and the Atmosphere. Johm Wiley & Sons, Chichester, UK, pp. 7–21.
Flechard, C.R., Ambus, P., Skiba, U., Rees, R.M., Hensen, A., van Amstel, A., van den Pol-van Dasselaar, A., Soussana, J.F., Jones, M., Clifton-Brown, J., Raschi, A., Horvath, L., Neftel, A., Jocher, M., Ammann, C., Leifeld, J., Fuhrer, J., Calanca, P., Thalman, E., Pilegaard, K., Di Marco, C., Campbell, C., Nemitz, E., Hargreaves, K.J., Levy, P.E., Ball, B.C., Jones, S.K., van de Bulk, W.C.M., Groot, T., Blom, M., Domingues, R., Kasper, G., Allard, V., Ceschia, E., Cellier, P., Laville, P., Henault, C., Bizouard, F., Abdalla, M., Williams, M., Baronti, S., Berretti, F., Grosz, B., 2007. Effects of climate and management intensity on nitrous oxide emissions in grassland systems across Europe. Agric. Ecosyst. Environ. 121, 135–152.
Flessa, H., Ruser, R., Schilling, R., Loftfield, N., Munch, J.C., Kaiser, E.A., Beese, F., 2002. N_2O and CH_4 fluxes in potato fields: automated measurements, management effects and temporal variation. Geoderma 105, 307–325.
Gillam, K.M., Zebarth, B.J., Burton, D.L., 2008. Nitrous oxide emissions from denitrification and the partitioning of gaseous losses as affected by nitrate and carbon addition and soil aeration. Can. J. Soil Sci. 88, 133–143.
Halvorson, A.D., Del Grosso, S.J., 2013. Nitrogen placement and source effects on nitrous oxide emissions and yields of irrigated corn. J. Environ. Qual. 42, 312–322.
Hutchinson, G.L., Mosier, A.R., 1981. Improved soil cover method for field measurement of nitrous oxide fluxes. Soil Sci. Soc. Am. J. 45, 311–316.
IPCC Climate Change, 2007. In: Solomon, S., et al. (Eds.), The Physical Science Basis. Cambridge University of Press.
Jacinthe, P.A., Dick, W.A., 1997. Soil management and nitrous oxide emissions from cultivated fields in southern Ohio. Soil Tillage Res. 41, 221–235.
Jarecki, M.K., Parkin, T.B., Chan, A.S.K., Hatfield, J.L., Jones, R., 2008. Comparison of DAYCENT-simulated and measured nitrous oxide emissions from a corn field. J. Environ. Qual. 37, 1685–1690.
Kemanian, A.R., Stöckle, C.O., 2010. C-Farm: a simple model to evaluate the carbon balance of soil profiles. Eur. J. Agron. 32, 22–29.
Liaw, A., Wiener, M., 2002. Classification and regression by randomForest. R. News 2, 18–22.
Liengaard, L., Figueiredo, V., Markfoged, R., Revsbech, N.P., Nielsen, L.P., Prast, A.E., Kühl, M., 2014. Hot moments of N_2O transformation and emission in tropical soils from the Pantanal and the Amazon (Brazil). Soil Biol. Biochem. 75, 26–36.

Ma, B.L., Wu, T.Y., Tremblay, N., Deen, W., Morrison, M.J., Mclaughlin, N.B., Gregorich, E.G., Stewart, G., 2010. Nitrous oxide fluxes from corn fields: on-farm assessment of the amount and timing of nitrogen fertilizer. Glob. Change Biol. 16, 156–170.
Mulla, D.J., Bhatti, A.U., Hammond, M.W., Benson, J.B., 1992. A comparison of winter wheat yield and quality under uniform vs. spatially variable fertilizer management. Agric. Ecosyst. Environ. 38, 301–311.
Oates, L.G., Duncan, D., Gelfand, I., Millar, N., Robertson, G.P., Jackson, R.D., 2016. Nitrous oxide emissions during establishment of eight alternative cellulosic bioenergy cropping systems in the North Central United States. Glob. Change Biol. Bioenergy 8, 539–549. http://dx.doi.org/10.1111/gcbb.12268.
Parkin, T.B., 2008. Effect of sampling frequency on estimates of cumulative N_2O emissions. J. Environ. Qual. 37, 1390–1395.
Parkin, T.B., Kaspar, T.C., 2006. Nitrous oxide emissions from corn-soybean systems in the Midwest. J. Environ. Qual. 35, 1496–1506.
Reeves, S., Wang, W., 2015. Optimum sampling time and frequency for measuring N_2O emissions from a rain-fed cereal cropping system. Sci. Total Environ. 530–531, 219–226.
Reeves, S., Wang, W., Salter, B., Halpin, N., 2016. Quantifying nitrous oxide emissions from sugarcane cropping systems: optimum sampling time and frequency. Atmos. Environ. 136, 123–133.
Regan, K., Kammann, C., Hartung, K., Lenhart, K., Muller, C., Philippot, L., Kandeler, E., Marhan, S., 2011. Can differences in microbial abundances help explain enhanced N_2O emissions in a permanent grassland under elevated atmospheric CO_2? Glob. Change Biol. 17, 3176–3186.
Rohatgi, A., 2012. WebPlotDigitizer: Web based tool to extract data from plots, images, and maps. Version 3.11. Website: http://arohatgi.info/WebPlotDigitizer (accessed on January 2017).
Saha, D., Rau, B.M., Kaye, J.P., Montes, F., Adler, P.R., Kemanian, A.R., 2016. Landscape control of nitrous oxide emissions during the transition from conservation reserve program to perennial grasses for bioenergy. Glob. Change Biol. Bioenergy. http://dx.doi.org/10.1111/gcbb.12395.
Smith, K.A., Dobbie, K.E., 2001. The impact of sampling frequency and sampling times on chamber-based measurements of N_2O emissions from fertilized soils. Glob. Change Biol. 7, 933–945.
Smith, K.A., Thomson, P.E., Clayton, H., Mctaggart, I.P., Conen, F., 2001. Effects of temperature, water content and nitrogen fertilization on emission of nitrous oxide by soils. Atmos. Environ. 32, 3301–3309.
Stöckle, C.O., Donatelli, M., Nelson, R., 2003. CropSyst, a cropping systems simulation model. Eur. J. Agron. 18, 289–307.
Stöckle, C.O., Kemanian, A.R., Kermer, C., 2008. On the use of radiation- and water-use efficiency for biomass production models. In: Ahuja, L., et al. (Eds.), Response of Crops to Limited Water: Understanding and Modeling Water Stress Effects on Plant Growth Processes. Advances in Agricultural Systems Modeling Ser. 1. ASA, CSSA, SSSA, Madison, WI, pp. 39–58.
Strobl, C., Malley, J., Tutz, G., 2009. An introduction to recursive partitioning: rational, application, and characteristics of classification and regression trees, bagging, and random forests. Psychol. Methods 14, 323–348.
Wagner-Riddle, C., Thurtell, G.W., 1998. Nitrous oxide emission from agricultural fields during winter and spring thaw as affected by management practices. Nutr. Cycl. Agroecosyst 52, 151–163.
White, C.M., Kemanian, A.R., Kaye, J.P., 2014. Implications of carbon saturation model structure for simulated nitrogen mineralization dynamics. Biogeosciences Discuss. 11, 9667–9695.
Zhang, J., Peng, C., Zhu, Q., Xue, W., Shen, Y., Yang, Y., Shi, G., Shi, S., Wang, M., 2016. Temperature sensitivity of soil carbon dioxide and nitrous oxide emissions in mountain forest and meadow ecosystems in China. Atmos. Environ. 142, 340–350.